Received: 30 October 2023 | Revised: 24 May 2024 | Accepted: 4 July 2024

DOI: 10.1111/apha.14202

ACTA PHYSIOLOGICA

RESEARCH PAPER

SPECIAL SERIES ON MITOCHONDRIAL BIOENERGETICS IN PHYSIOLOGY

HIF-1α limits myocardial infarction by promoting mitophagy in mouse hearts adapted to chronic hypoxia

Petra Alanova[1] | **Lukas Alan**[2,3] | **Barbora Opletalova**[1,4] | **Romana Bohuslavova**[5] | **Pavel Abaffy**[6] | **Katerina Matejkova**[5] | **Kristyna Holzerova**[1] | **Daniel Benak**[1] | **Nina Kaludercic**[7,8,9] | **Roberta Menabo**[8] | **Fabio Di Lisa**[7,8] | **Bohuslav Ostadal**[1] | **Frantisek Kolar**[1] | **Gabriela Pavlinkova**[5]

[1]Laboratory of Developmental Cardiology, Institute of Physiology of the Czech Academy of Sciences, Prague, Czech Republic

[2]Laboratory of Bioenergetics, Institute of Physiology of the Czech Academy of Sciences, Prague, Czech Republic

[3]Department of Biology, University of Padova, Padova, Italy

[4]Faculty of Science, Charles University, Prague, Czech Republic

[5]Laboratory of Molecular Pathogenetics, Institute of Biotechnology, Czech Academy of Sciences, Vestec, Czechia

[6]Laboratory of Gene Expression, Institute of Biotechnology, Czech Academy of Sciences, Vestec, Czechia

[7]Department of Biomedical Sciences, University of Padova, Padova, Italy

[8]Neuroscience Institute, National Research Council of Italy (CNR), Padova, Italy

[9]Fondazione Istituto di Ricerca Pediatrica Città della Speranza (IRP), Padova, Italy

Correspondence
Petra Alanova, Laboratory of Developmental Cardiology, Institute of Physiology of the Czech Academy of Sciences, Vídeňská 1083, 142 20 Praha 4, Czech Republic.
Email: petra.alanova@fgu.cas.cz

Gabriela Pavlinkova, Laboratory of Molecular Pathogenetics, Institute of Biotechnology, Czech Academy of Sciences, Průmyslová 595, 252 50 Vestec, Czechia.
Email: gabriela.pavlinkova@ibt.cas.cz

Funding information
National Institute for Research of Metabolic and Cardiovascular Diseases, Grant/Award Number: LX22NPO5104; Ministry of Health of the Czech Republic, Grant/Award Number: NU20J-02- 00035; Charles University, Grant/Award Number: 270623; European Union–Next Generation EU; National Recovery and Resilience

Abstract

Aim: The transcriptional factor HIF-1α is recognized for its contribution to cardioprotection against acute ischemia/reperfusion injury. Adaptation to chronic hypoxia (CH) is known to stabilize HIF-1α and increase myocardial ischemic tolerance. However, the precise role of HIF-1α in mediating the protective effect remains incompletely understood.

Methods: Male wild-type (WT) mice and mice with partial *Hif1a* deficiency (*hif1a*$^{+/-}$) were exposed to CH for 4 weeks, while their respective controls were kept under normoxic conditions. Subsequently, their isolated perfused hearts were subjected to ischemia/reperfusion to determine infarct size, while RNA-sequencing of isolated cardiomyocytes was performed. Mitochondrial respiration was measured to evaluate mitochondrial function, and western blots were performed to assess mitophagy.

Results: We demonstrated enhanced ischemic tolerance in WT mice induced by adaptation to CH compared with their normoxic controls and chronically hypoxic *hif1a*$^{+/-}$ mice. Through cardiomyocyte bulk mRNA sequencing analysis, we unveiled significant reprogramming of cardiomyocytes induced by CH

Petra Alanova and Lukas Alan co-first authors.

Plan (NRRP), Grant/Award Number: C93C22007550006; Czech Academy of Sciences, Grant/Award Number: RVO: 86652036

emphasizing mitochondrial processes. CH reduced mitochondrial content and respiration and altered mitochondrial ultrastructure. Notably, the reduced mitochondrial content correlated with enhanced autophagosome formation exclusively in chronically hypoxic WT mice, supported by an increase in the LC3-II/LC3-I ratio, expression of PINK1, and degradation of SQSTM1/p62. Furthermore, pretreatment with the mitochondrial division inhibitor (mdivi-1) abolished the infarct size-limiting effect of CH in WT mice, highlighting the key role of mitophagy in CH-induced cardioprotection.

Conclusion: These findings provide new insights into the contribution of HIF-1α to cardiomyocyte survival during acute ischemia/reperfusion injury by activating the selective autophagy pathway.

KEYWORDS

cardioprotection, chronic hypoxia, hypoxia-inducible factor 1 alpha, mitochondria, mitophagy, myocardial infarction

1 | INTRODUCTION

Adaptation to chronic hypoxia (CH) is known to protect the heart against acute ischemia/reperfusion (I/R) injury. In line with the human epidemiological surveys,[1,2] the vast majority of animal studies demonstrated that CH confers the protective long-lasting phenotype against major endpoints of acute I/R injury (reviewed in[3]). CH also induces remodeling of the pulmonary vasculature, leading to pulmonary hypertension and right ventricle (RV) hypertrophy.[4] Hypoxia-inducible factor 1 (HIF-1) is a critical oxygen-sensitive transcription factor that mediates the body's adaptive responses to hypoxia through the activation of more than 800 target genes that are involved in many different cellular processes, such as cell proliferation, angiogenesis, erythropoiesis, metabolism, and apoptosis.[5] Heterodimer HIF-1 consists of two subunits – HIF-1α and HIF-1ß (aryl hydrocarbon translocator). Whereas α and ß-subunits are constitutively expressed, the protein stability of the α-subunit is regulated in accordance with cellular O_2 level.[6] Under normoxic conditions, the α-subunit is rapidly degraded by 2-oxoglutarate-dependent prolyl-4-hydroxylases. During hypoxia, the activity of prolyl hydroxylases becomes inhibited, allowing the α-subunit to accumulate, heterodimerize with ß-subunit, and initiate the transcription.[7]

Several studies demonstrated that HIF-1α is necessary for the acute phase of cardiac protection by ischemic preconditioning (IPC[8];; as well as for remote IPC[9]). In contrast to classic IPC, CH-induced cardiac protection persists much longer than those provided by any form of conditioning.[10] Moreover, CH not only activates protective signaling pathways but also affects the expression of their components and other proteins associated with the maintenance of oxygen homeostasis via HIF-1α.[11] Mitochondria are a key part of cell signaling network, responsible for oxygen handling in cardiac myocytes; therefore, it is not surprising that CH-induced adaptive changes affect also mitochondrial function.[12] Mitochondria have emerged as the critical targets and key mediators of cell death when the heart is subjected to ischemia and subsequent reperfusion. Mitochondria account for over 30% of cardiomyocyte volume to meet the constant high energy demand.[13] They are not only responsible for adenosine triphosphate (ATP) production but also participate in many other physiological functions, such as calcium handling,[14] cell signaling, and production of reactive oxygen species (ROS).[15] Therefore, mitochondrial quality control plays an important role in maintaining cellular homeostasis and cell survival. We previously found that several mitochondrial components are involved in the protective mechanism of CH.[16,17]

Removal of damaged mitochondria is mediated by mitochondrial selective macroautophagy/autophagy.[18] Once initiated, mitophagy is mediated by sequestration of targeted mitochondria into a double-membrane autophagosomes (AP) fusing with lysosomes to ensure their degradation and recycling.[19] However, the role of mitophagy in cardioprotection induced by CH and more specifically its connection with HIF-1α has not been

studied yet. Here, we focused on the impact of partial *Hif1a* deficiency on myocardial ischemic tolerance and mitochondrial function.

2 | RESULTS

2.1 | Right ventricle hypertrophy induced by chronic hypoxia depends on HIF-1α

Wild-type (WT) mice and mice with partial *Hif1a* deficiency (*hif1a*$^{+/-}$) were adapted to CH to explore their physiological responses (Figure 1A). Adaptation to CH caused a mild growth retardation expressed by decreased body weight in both WT and *hif1a*$^{+/-}$ mice compared to their normoxic counterparts. As expected, our hypoxic protocol led to increased relative RV weight in WT mice; however, the effect was absent in chronically hypoxic *hif1a*$^{+/-}$ mice indicating that HIF-1α is necessary for development of hypoxia-induced RV hypertrophy. There were no significant differences in left ventricle (LV) weight among the experimental groups (Table 1). As expected, adaptation to CH induced polycythemia demonstrated by significantly increased level of hematocrit in both CH groups compared to their corresponding normoxic controls. This increase was more pronounced in WT mice than in *hif1a*$^{+/-}$ mice (Table S1).

2.2 | HIF-1α is necessary for cardiac protection induced by chronic hypoxia

To assess whether partial *Hif1a* deficiency affects the increased ischemic tolerance induced by adaptation to CH, we challenged the hearts of both normoxic and chronically hypoxic WT and *hif1a*$^{+/-}$ mice with acute I/R insult. Isolated perfused hearts were subjected to global I/R injury for infarct size (IS) determination. The results confirmed the cardioprotective effect of CH,[2,20] as WT mice demonstrated reduced IS compared to their normoxic counterparts. On the other hand, adaptation to CH had no protective effect in *hif1a*$^{+/-}$ mice suggesting that partial *Hif1a* deficiency blunted the development of cardioprotective phenotype provided by CH (Figure 1B,C).

2.3 | Chronic hypoxia-induced changes in the transcriptome of cardiomyocytes

To gain insights at the molecular level on how CH and *Hif1a* mutation affect cardiomyocytes, we performed RNA

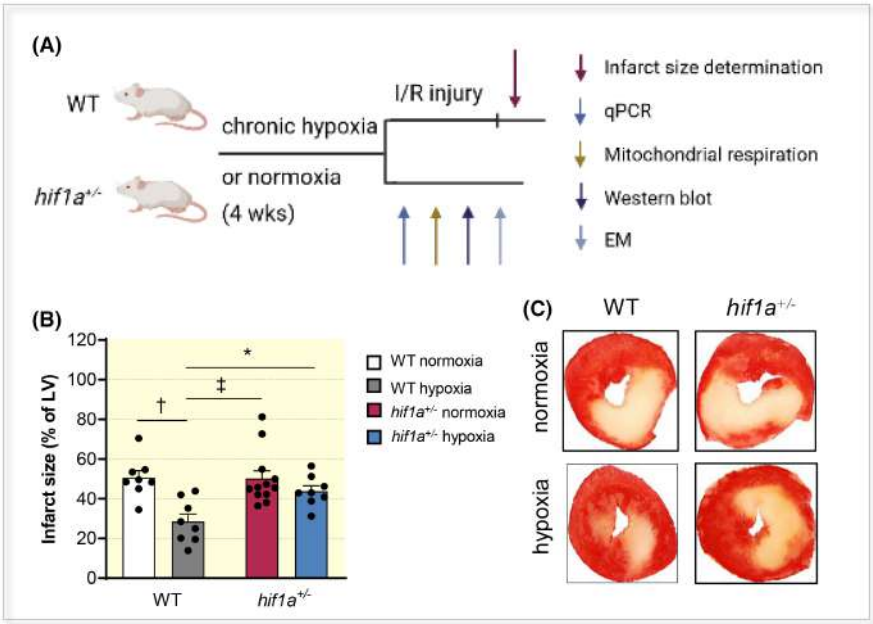

FIGURE 1 Partial *Hif1a* deficiency inhibits CH-induced myocardial protection against I/R injury. (A) Experimental design: WT and *hif1a*$^{+/-}$ mice were adapted to CH or kept in normoxia for 4 weeks. At the end of the adaptation period, all four experimental groups were (i) subjected to I/R injury for infarct size determination or (ii) their LV were collected for different analyses. Created with BioRender.com. (B) Infarct size normalized to the size of LV of normoxic and chronically hypoxic WT and *hif1a*$^{+/-}$ mice. Values are means ± SEM, $n = 8–12$ mice per group. *$p < 0.05$, †$p < 0.01$, ‡$p < 0.001$, two-way ANOVA with Bonferroni's multiple comparisons test. (C) Representative images of histochemically stained cross sections of the hearts from normoxic and chronically hypoxic WT and *hif1a*$^{+/-}$ mice. Red represents survived tissue, and white represents infarction.

TABLE 1 Changes in body and heart weight.

Group		*n*	BW [g]	LV [mg]	LV/BW [mg/g]	RV [mg]	RV/BW [mg/g]	HW [mg]	HW/BW [mg/g]
Normoxia	WT	10	29.31 ± 2.95	58.87 ± 2.98	2.00 ± 0.09	22.69 ± 1.27	0.77 ± 0.05	106.07 ± 3.27	3.61 ± 0.10
	hif1a$^{+/-}$	23	27.46 ± 0.47	55.18 ± 1.18	2.02 ± 0.05	21.85 ± 0.70	0.80 ± 0.03	99.57 ± 1.56	3.64 ± 0.06
Hypoxia	WT	12	26.27 ± 0.39*	48.46 ± 1.03	1.89 ± 0.04	23.88 ± 0.51	0.93 ± 0.02*	93.09 ± 1.27	3.63 ± 0.05
	hif1a$^{+/-}$	21	25.38 ± 0.47*	50.03 ± 1.10	1.96 ± 0.04	20.35 ± 0.60	0.80 ± 0.02#	91.62 ± 1.65	3.59 ± 0.05

Note: CH induced changes in body and heart weight. Values are means ± SEM from the indicated number of animals (*n*) in each group. *$p < 0.05$ versus corresponding normoxic group; #$p < 0.05$ versus corresponding WT group, two-way ANOVA with Bonferroni's multiple comparisons test.

Abbreviations: BW, body weight; LV, left ventricle; RV, right ventricle; HW, heart weight.

sequencing of cardiomyocytes isolated from the LV of normoxic and chronically hypoxic WT and *hif1a*$^{+/-}$ mice (Figure 2A). The clustering analysis of transcriptomes from hypoxic and normoxic WT and *hif1a*$^{+/-}$ cardiomyocytes indicates that the effect of CH exposure is more pronounced than the influence of genotype (Figure 2B). This finding is further supported by the consistent clustering patterns observed in the relative mRNA levels of selected genes, which were verified through qRT-PCR analysis using RNA isolated from the LV (Figure 2C, Figure S1). Compared to normoxic WT cardiomyocytes, 606 and 737 protein-coding genes were differentially expressed in chronically hypoxic WT and *hif1a*$^{+/-}$ cardiomyocytes, respectively ($p < 0.05$ and 30%-fold change threshold; Figure 2D–F, Table S2). Of these, 387 transcripts were found in both chronically hypoxic WT and *hif1a*$^{+/-}$ cardiomyocytes. The comparison of transcriptomes of hypoxic WT and *hif1a*$^{+/-}$ cardiomyocytes identified of 80 transcripts differentially expressed (Figure 2G, Table S2). Functional profiling of differentially expressed genes in hypoxic WT and *hif1a*$^{+/-}$ cardiomyocytes revealed that the top gene clusters were related to highly enriched biological pathways and specific gene ontology (GO) term categories associated with biological oxidations, response to stress, vasculature, extracellular matrix, and metabolism, indicating similar structural and functional hypoxia-induced remodeling (Figure 2H, Table S3). Shared upregulated genes in chronically hypoxic WT and *hif1a*$^{+/-}$ cardiomyocytes encoding enzymes associated with oxidative stress included glutathione peroxidases, glutathione S-transferases, monoamine oxidases (*Gstt1*, *Gstt2*, *Gstt3*, *Gpx3*, *Mgst1*, *Maoa*, and *Maob*), apoptosis (*Casp3*), and metabolism (*Pck2*, *Pdk4*, *Acat2*, *Aldob*, and *Prkd1*). Pathway enrichment analysis identified PI3K-Akt signaling pathway, HIF-1 signaling, and Focal Adhesion-PI3K-Akt–mTOR-signaling pathway associated with down-regulated genes in both hypoxic WT and *hif1a*$^{+/-}$ groups, including *Vegfa*, *Egln3*, *Cdkn1a*, *Nppa*, *Fgf6*, *Col4a1*, *Tlr4*, and *Thbs1*. We focused on the transcriptome comparison between chronically hypoxic WT and *hif1a*$^{+/-}$ cardiomyocytes to reveal specific differences in cellular responses. Notably, compared to hypoxic WT, hypoxic *hif1a*$^{+/-}$ cardiomyocytes exhibited downregulation of key genes such as anti-apoptotic *Bcl2* that regulates cell death by controlling the mitochondrial membrane permeability[21]; *Pfkfb4* (HIF-1 target gene) encoding glycolytic enzyme associated with a metabolic switch in cardiomyocytes[22]; *Myc*, regulating glucose metabolism and mitochondrial biogenesis in response to pathologic stress[23]; *Egr1*, the transcription factor early growth response-1, associated with ischemic pathology and cardiac hypertrophy[24]; and the transcription activator *Stat3* mediating mitochondrial metabolism and cardioprotective

processes against I/R injury.[25] Conversely, chronically hypoxic *hif1a*$^{+/-}$ cardiomyocytes exhibited upregulation of certain genes, including glutathione peroxidase 1 (*Gpx1*), *Casp3* enzyme of the apoptotic pathway, neuregulin 4 (*Nrg4*), and *Fabp4* and *Fabp5* encoding fatty acid-binding proteins. *Gpx1* prevents cardiac mitochondrial dysfunction associated with reoxygenation following I/R injury[26]; *Nrg4* is associated with the activation of autophagy through the AMPK/mTOR-dependent signaling pathway[27]; and *Fabp4* and *Fabp5* are connected to cardiac pathological remodeling and mitochondrial function.[28,29] In summary, the comparison of transcriptomes of chronically hypoxic WT and *hif1a*$^{+/-}$ cardiomyocytes revealed specific gene expression changes, involving cell death regulation, metabolism, cardiac remodeling, autophagy, mitochondrial metabolism, and mitochondrial dysfunction prevention.

2.4 | Chronic hypoxia reduces mitochondrial respiration and mass via HIF-1α

Based on the results obtained from cardiomyocytes bulk mRNA-sequencing, we decided to investigate whether adaptation to CH has an impact on mitochondria and to clarify the possible role of HIF-1α. We measured mitochondrial respiration and performed gene and protein analyses. As shown in Figure 3A, adaptation to CH was accompanied by a significant decline in mitochondrial state 3 respiration in WT mice heart homogenates. However, the uncoupled control ratio (Figure S2) was unchanged indicating proper function of the respiratory chain. Mitochondrial mass was evaluated by measuring mitochondrial deoxynucleic acid (mtDNA) copy number. Changes in mtDNA content were related to the number of copies of a mitochondrial gene *Mtatp6* and the number of copies of a nuclear gene *Nme1* using quantitative PCR (qPCR; Tables S4 and S5). We revealed a marked reduction of the mtDNA content in the LV tissue of chronically hypoxic WT mice compared to their normoxic controls. The mtDNA content remained unchanged in both normoxic and chronically hypoxic *hif1a*$^{+/-}$ mice (Figure 3B). To verify the decreased CH-induced mitochondrial mass, we performed western blot analysis of mitochondrially encoded protein cytochrome *c* oxidase 1 (COX1) in relation to classical cellular protein loading marker vinculin. These data revealed decreased COX1 expression in chronically hypoxic WT mice only (Figure 3C). These findings indicate that HIF-1α regulates mitochondrial processes in cardiac myocytes during adaptation to CH.

2.5 | Changes in mitochondrial ultrastructure in chronically hypoxic hearts depend on HIF-1α

Heart mitochondria were investigated by transmission electron microscopy (TEM). The electron micrographs were acquired from the LV of the normoxic and chronically hypoxic WT and *hif1a*$^{+/-}$ mice. Alterations in size and distribution of mitochondria are evident (Figure 3D). The average mitochondrial size was increased in hypoxic WT group only (Figure 3E). These changes were significant compared to the normoxic control group and were absent in chronically hypoxic *hif1a*$^{+/-}$ mice. More detailed quantitative analysis revealed a reduced proportion of small mitochondria in favor of larger mitochondria in the hearts of chronically hypoxic WT mice (Figure 3F).

2.6 | HIF-1α mediates chronic hypoxia-induced mitophagy

To explain the presence of the higher number of larger mitochondria with simultaneous reduction in mitochondrial mass in LV samples of chronically hypoxic WT mice, we hypothesized that autophagy/mitophagy might have occurred. Mitophagy is responsible for degradation of redundant or damaged mitochondria via their sequestration into AP. We performed microtubule-associated light chain protein 3 (LC3) assay to monitor autophagic flux. It was defined as the increase in lipidated LC3-II on western blot analysis after the addition of lysosomal inhibitor leupeptin. Adaptation to CH led to a significant increase in the LC3-II/LC3-I ratio after the leupeptin administration in WT mice suggesting the increased AP formation (Figure 4A). Sequestosome 1 (SQSTM1/p62) is an essential adaptor protein with the ability to identify and deliver polyubiquitinated organelles to AP for degradation.[30] We assessed the protein level of SQSTM1/p62 as an alternative method for detecting the autophagic flux. Since SQSTM1/p62 directly interacts with LC3,[30] its sequestration reflects autophagy. We observed a decreased level of SQSTM1/p62 after the adaptation to CH in WT mice compared to their normoxic counterparts as well as to chronically hypoxic *hif1a*$^{+/-}$ mice (Figure 4B). Finally, we verified the protein expression of PTEN-induced putative kinase 1 (PINK1). Normally, PINK1 is imported to the inner mitochondrial membrane, where it is subsequently cleaved by several proteases.[31] However, the loss of mitochondrial membrane potential prevents its import, resulting in the accumulation of unprocessed PINK1 at the outer mitochondrial membrane. This accumulation recruits Parkin from the cytosol to damaged mitochondria initiating autophagy

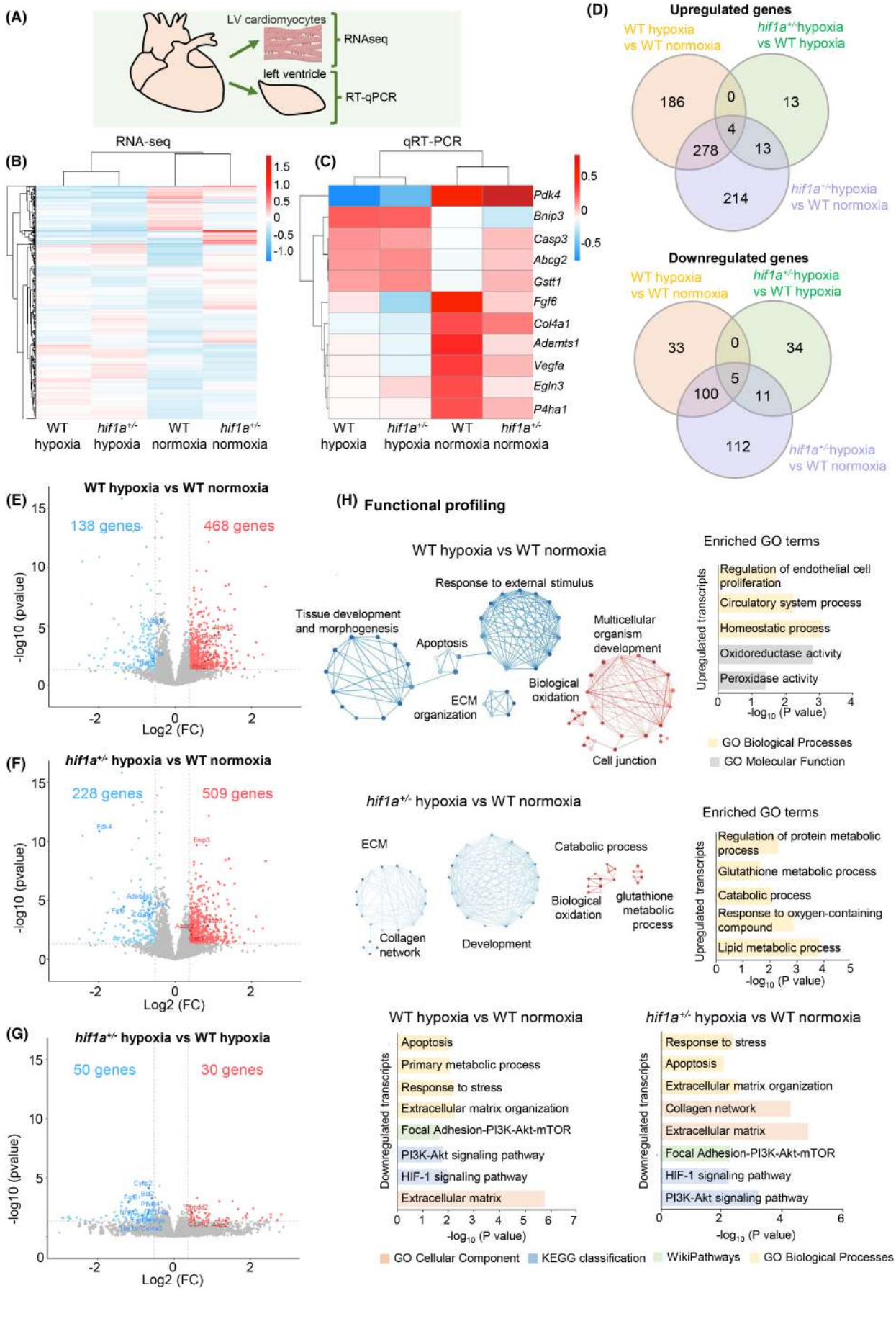

activation.[32] We observed an increase in PINK1 level after adaptation to CH in the LV myocardium from WT but not from *hif1a*$^{+/-}$ mice (Figure 4C) suggesting that HIF-1α mediated mitophagy in a PINK1/Parkin-dependent pathway. To test the hypothesis that HIF-1α-dependent reduction of mitochondrial mass is processed through autophagy, we created *Atg7* knockout (KO) cells on the AC16 human cardiomyocyte cell line background and transfected them with either proline hydroxylases resistant HIF-1α plasmid[33] simulating chronically hypoxic conditions or empty vector (EV). Transfection efficiency was confirmed by the increased protein expression of lactate dehydrogenase A (LDHA, Figure 4D,F), a direct HIF-1 target.[34] Autophagy related 7 (ATG7) is a key autophagy protein that drives the conjugation of phosphatidylethanolamine to LC3-I generating LC3-II, which is found on AP membranes.[35] We demonstrated that HIF-1α overexpression resulted in markedly decreased protein expression of mitochondrial ATP synthase subunit beta (ATP5B), a marker of mitochondrial mass, in WT cells compared to EV transfected cells (Figure 4E,F). Thus, these data confirmed the presence of HIF-1α-driven mitochondrial degradation.

2.7 | HIF-1α-activated mitophagy is essential for induction of cardioprotective phenotype

To confirm whether the cardioprotective effect of CH depends on mitophagy activated by HIF-1α, we performed another set of experiments as a proof of principle. Since mitochondrial fragmentation is considered a prerequisite for mitophagy,[36] we pharmacologically inhibited mitophagy using mitochondrial division inhibitor (mdivi-1) that targets DRP1.[37] We pretreated both normoxic and chronically hypoxic WT and *hif1a*$^{+/-}$ mice with mdivi-1 and challenged their hearts with acute myocardial infarction for IS determination. The results demonstrated that the cardioprotective effect of CH in WT mice was abolished by mitophagy inhibition (Figure 5A). These data indicate that HIF-1α drives mitophagy, which is essential for protection of the heart against I/R injury (graphically depicted in Figure 5B).

3 | DISCUSSION

In the present study, we evaluated whether HIF-1α signaling is involved in CH-induced mitophagy and whether this process plays a protective role against myocardial I/R injury. We found that (i) cardioprotection is HIF-1α-dependent as mice with partial *Hif1a* deficiency did not develop an increased ischemic tolerance after adaptation to CH; (ii) adaptation to CH was associated with HIF-1α-induced cardiomyocyte reprogramming pointing at the altered mitochondrial function; and (iii) the CH-induced cardioprotection depended on mitophagy activated by HIF-1 pathway. Therefore, the major novel finding of our study is that HIF-1α is essential for induction of mitophagy, which is a necessary prerequisite for cardioprotection induced by CH in mice.

The most frequently used experimental model in research on chronic high-altitude hypoxia is hypoxia simulated under laboratory conditions in a hypoxic chamber. Chronic hypoxia is not always a continuous state; it is frequently of intermittent nature (repeated ascents in mountains, sleep apnea). Likewise, hypoxia during myocardial ischemia is not continuous but is dependent on regional coronary blood flow dynamics.[3] Experimental data comparing the effects of permanent and intermittent CH on the myocardium are sporadic. In addition, experimental protocols of intermittent hypoxia vary greatly in cycle length, severity, and number of hypoxic episodes. These factors are critical in

FIGURE 2 Hypoxia-mediated reprogramming of WT and *hif1a*$^{+/-}$ cardiomyocytes. (A) Experimental design: Cardiomyocytes were isolated from the LV of normoxic and chronically hypoxic WT and *hif1a*$^{+/-}$ hearts and used for bulk RNA-seq analyses. For validation experiments, RNA was isolated from the LV and used in qRT-PCR validation of selected genes identified in RNA-seq. (B) Clustering analyses of differentially expressed genes (cutoff the *p* value <0.05 and FC > 30%) among four conditions based on expression profiles in RNA-seq. (C) Heatmap of expression of selected genes identified in RNA-seq and analyzed by qRT-PCR. (D) Venn diagrams comparing differentially expressed transcripts across LV cardiomyocytes, mapping intergroup comparisons. (E) Volcano plot of transcriptomic changes between hypoxic and normoxic WT cardiomyocytes; colored dots correspond to genes with significant changes (cutoff the adjusted *p*-value <0.05 and FC > 30%). The complete list of identified down- and up-differentially expressed genes is in Table S2. (F) Volcano plot of transcriptomic changes between hypoxic *hif1a*$^{+/-}$ and normoxic WT cardiomyocytes. The complete list of identified down- and up-differentially expressed genes is in Table S2. (G) Volcano plot of transcriptomic changes between hypoxic *hif1a*$^{+/-}$ and hypoxic WT cardiomyocytes. The complete list of identified down- and up-differentially expressed genes is in Table S2. (H) Functional profiling analysis of differentially downregulated or upregulated transcripts in hypoxic cardiomyocytes. Enrichment maps of down- and upregulated gene ontology (GO) sets visualized by the network between hypoxic WT or hypoxic *hif1a*$^{+/-}$ and normoxic WT cardiomyocytes. Each node represents a GO term; edges depict shared genes between nodes. Each GO set cluster was assigned with representative keywords. Bar graphs show the enriched GO terms and pathways for up- and downregulated transcripts in WT or *hif1a*$^{+/-}$ hypoxic cardiomyocytes; a list of GO sets is available in Table S3.

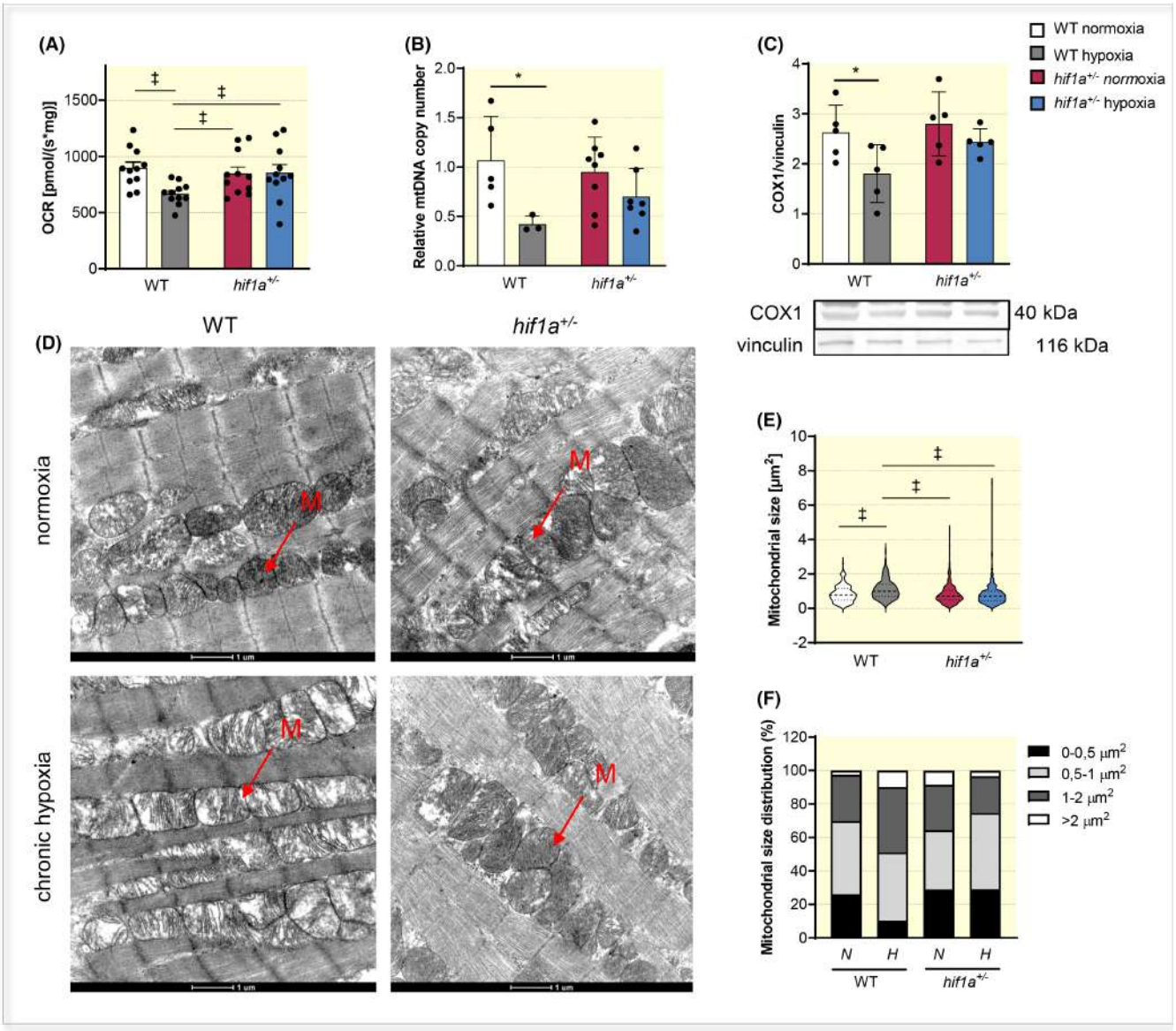

FIGURE 3 CH reduces mitochondrial content, function and alters its ultrastructure. (A) Mitochondrial oxygen consumption rate (OCR) in heart homogenates of normoxic and chronically hypoxic WT and *hif1a*$^{+/-}$ mice; $n = 11$ mice per group. (B) Mitochondrial DNA copy number in LV tissue of normoxic and chronically hypoxic WT and *hif1a*$^{+/-}$ mice; $n = 3$–7 mice per group. (C) Protein expression of COX1 normalized to vinculin in LV tissue of normoxic and chronically hypoxic WT and *hif1a*$^{+/-}$ mice; $n = 5$ mice per group. (D) Representative transmission electron micrographs of LV of the indicated group with arrows pointing to mitochondria; scale bar: 1 µm. (E) Mean mitochondrial size in LV myocardium; $n = 491$ analyzed mitochondria per group and (F) Distribution of mitochondrial size of normoxic and chronically hypoxic WT and *hif1a*$^{+/-}$ mice. Values are means ± SEM (A) or SD (B, C); $^{*}p < 0.05$, $^{‡}p < 0.001$, two-way ANOVA with Bonferroni's (A, B, E) or Sidak's (C) multiple comparisons test.

determining whether intermittent hypoxia is beneficial or harmful.[38] The adaptation to chronic intermittent hypobaric hypoxia, used in this study, represents a well-defined and reproducible protocol improving cardiac ischemic tolerance.[39,40] Despite the well-known infarct size-limiting effect of CH that has been recognized for many decades,[2] the specific question regarding whether HIF-1 itself confers this protective phenotype has not been addressed until now. Therefore, we analyzed the effect of genetically and functionally modified levels of HIF-1α in isolated perfused hearts of WT and *hif1a*$^{+/-}$ mice adapted to CH. We found that myocardial infarction was significantly smaller in chronically hypoxic WT mice compared to their normoxic counterparts. This result aligns with the findings in our previous studies.[10,20] Interestingly, this effect of CH was absent in mice with partial *Hif1a* deficiency. Thus, the novel finding is that HIF-1 mediates not only the body's response to hypoxia, but it is also a decisive factor for the infarct size. The explanation could lie in HIF-dependent expression of

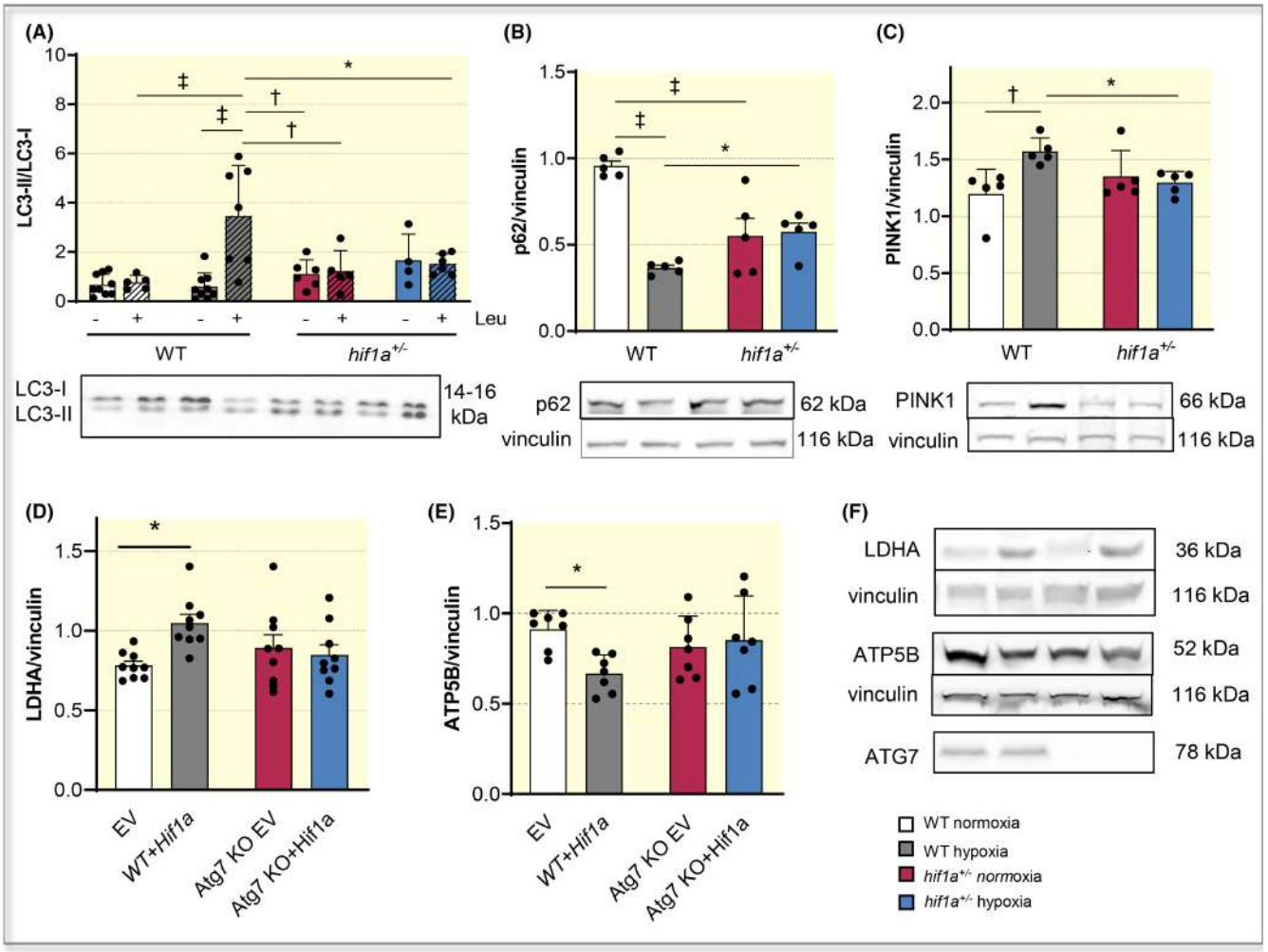

FIGURE 4 CH induces autophagic flux. (A) LC3-II/LC3-I ratio in LV of normoxic and chronically hypoxic WT and *hif1a*$^{+/-}$ mice administered with PBS/leupeptin. Values are means ± SD; $n = 4$–9 mice per group. *$p < 0.05$, $^{\dagger}p < 0.01$, $^{\ddagger}p < 0.001$, three-way ANOVA with Bonferroni's multiple comparisons test. (B) Protein expression of SQSTM1/p62 normalized to vinculin, (C) Protein expression of PINK1 normalized to vinculin in LV of normoxic and chronically hypoxic WT and *hif1a*$^{+/-}$ mice. Values are means ± SD; $n = 5$ mice per group. *$p < 0.05$, $^{\dagger}p < 0.01$, $^{\ddagger}p < 0.001$, two-way ANOVA with Bonferroni's multiple comparisons test. (D) Protein expression of LDHA normalized to vinculin. Values are means ± SEM; $n = 9$. *$p < 0.05$, two-way ANOVA with Bonferroni's multiple comparisons test. (E) Protein expression of ATP5B normalized to vinculin. Values are means ± SD; $n = 7$. *$p < 0.05$, two-way ANOVA with Bonferroni's multiple comparisons test. (F) Representative western blots in WT cells and *Atg7* KO cells with HIF-1α overexpression or with empty vector (EV).

genes enhancing the capacity for ATP generation by metabolic switch toward anaerobic glycolysis, regulating local O_2 supply by myocardial angiogenesis and increasing antioxidant capacity. Zhang et al.[41] studied the reprogramming induced by CH and depicted the crucial role of mitofusin 2 being involved in the regulation of mitochondrial fusion and cell metabolism. HIF-1α was demonstrated to exert a protective role in renal I/R injury through increased expression of HIF-1-targeted genes involved in the shift of glucose metabolism to glycolysis.[42] Cai et al.[43] demonstrated that delayed protection against myocardial ischemia induced by hypoxic preconditioning (5 cycles, 6% O_2, 5 min + 21% O_2, 5 min) was lost in *hif1a*$^{+/-}$ mice. Several studies demonstrated that HIF-1α is necessary for the acute phase of IPC[8] as well as for remote IPC,[9] since a partial *Hif1a* deficiency was associated with a complete loss of protection against I/R injury. In addition, ischemic or pharmacological postconditioning markedly increased mRNA and protein expression of *Hif1a* gene in ischemic tissue after reperfusion.[44,45]

In line with other studies,[46,47] we showed decreased mitochondrial content in LV tissue and cardiomyocytes after exposure to CH. Zhang et al.[48] reported decreased mtDNA mass in WT mouse embryonic fibroblasts (MEFs) exposed to 1% O_2 for 48 h compared to *hif1a*$^{-/-}$ MEFs. Based on our results, we propose that the decrease in mitochondrial content is an adaptive response

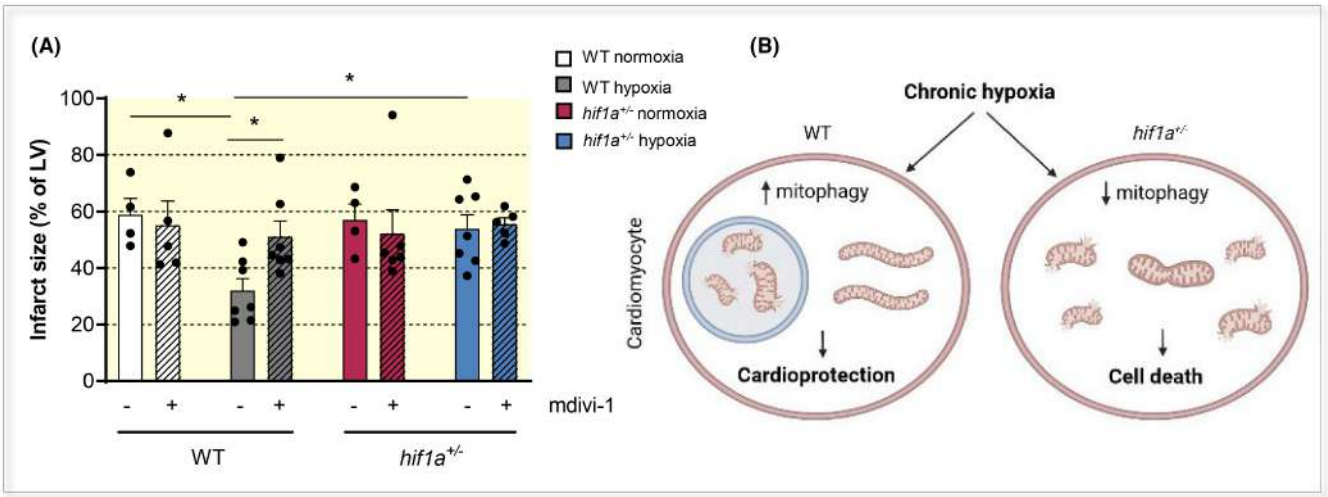

FIGURE 5 CH-induced mitophagy is HIF-1α driven. (A) The IS normalized to the size of LV of the hearts from normoxic and chronically hypoxic WT and *hif1a*$^{+/-}$ mice administered with DMSO/mdivi-1. Values are means ± SD, $n = 4–7$ mice per group. *$P < 0.05$, three-way ANOVA with Bonferroni's multiple comparisons test. (B) Graphical summary showing the consequences of *Hif1a* loss on mitochondrial function and cardioprotection induced by adaptation to CH. Created with BioRender.com.

that safeguards cells against the excessive generation of ROS under conditions of reduced oxygen availability. In cardiomyocytes, the largest amount of ROS is generated within the mitochondria.[49] The mitochondrial respiratory chain is the best-characterized source of ROS production; however, monoamine oxidases (MAO), outer mitochondrial membrane enzymes, have been shown to produce more H_2O_2 than the mitochondrial respiratory chain.[50] The role of MAO has been proved in cardiac pathologies such as I/R injury,[51] heart failure,[52,53] diabetic cardiomyopathy,[54,55] or doxorubicin-induced cardiotoxicity.[56] Through RNA-sequencing, we observed an increase in *Maoa and Maob* gene expression in chronically hypoxic mice (Table S2). Our group previously reported that adaptation to chronic intermittent hypoxia is associated with ROS generation, enhancing cardiac tolerance against acute I/R injury.[57,58] While the precise site of ROS generation remains unknown, we hypothesize that ROS act as a second messenger, and ROS moderate levels are necessary for the improved ischemic tolerance induced by CH.

Interestingly, together with decreased mitochondrial content, we observed an increased size of mitochondria in chronically hypoxic WT mice. Mitochondrial fission stimulated by DRP1 phosphorylation on Ser616 has been described as essential for segregation of damaged mitochondria.[59] Conversely, mitochondria elongate as a result of DRP1 phosphorylation at Ser637 by PKA, which is triggered by an increase in cyclic adenosine monophosphate levels. Gomes et al.[60] demonstrated that during starvation activated PKA phosphorylates DRP1 at Ser637, allowing mitochondrial fusion in mouse embryonic fibroblasts. As fragmented mitochondria are usually associated with apoptosis, the elongated mitochondria are thought to be more bioenergetically efficient.[61] The elongated mitochondria possess various advantageous features, such as resistance to autophagic degradation, an increased number of cristae, enhanced dimerization and activity of ATP synthase, and sustained ATP production, enabling the survival of starving cells.[62] As hypoxia increases activity of PKA[63] and HIF-1 represses mitochondrial biogenesis,[64] we hypothesized that fragmented mitochondria were sequestered by mitophagy leaving the larger elongated mitochondria with a maintained function. Our hypothesis further correlated with the respiration data showing a decrease in coupled respiration in the whole heart homogenates of chronically hypoxic WT mice, while the uncoupled control ratio did not show any difference. Therefore, we conclude that CH-induced decrease in mitochondrial respiration can be explained by the loss of mitochondrial mass, without affecting quality of remaining mitochondria.

Accumulated data show that mitophagy plays a pivotal role in maintaining cellular homeostasis in the heart, and the elimination of possibly dysfunctional mitochondria is a key determinant in the progression of myocardial I/R injury.[65,66] Therefore, we hypothesized that mitophagy is HIF-1-dependent and involved in the regulation of cardiac tolerance to I/R injury. To evaluate mitophagy, we assessed significantly increased autophagic flux in WT mice adapted to CH compared to their normoxic controls and chronically hypoxic *hif1a*$^{+/-}$ mice. Autophagy activation was confirmed by alterations in the protein abundance of SQSTM1/p62, a well-studied autophagy substrate that directly binds to LC3 and is degraded by autophagy, and PINK1 that accumulates in response to mitochondrial

membrane depolarization and damage. The connection between HIF-1 and autophagy has been previously described in pancreatic cancer cells[67] and human umbilical vein endothelial cells[68] exposed to hypoxia. Additionally, we also observed an increased *Bnip3* in chronically hypoxic WT mice compared to their normoxic controls (Figure 2C and Figure S1). BNIP3, a downstream HIF-1 target, is known to trigger mitochondrial autophagy as part of the adaptive metabolic response to hypoxia.[69] Previous studies demonstrated HIF-1-dependent induction of BNIP3 leading to mitophagy under prolonged (48 h) hypoxia in MEFs.[48] Moreover, BNIP3 binds to LC3,[70] supporting the involvement of BNIP3 in HIF-1α-activated mitophagy observed in our study.

Our bulk mRNA sequencing analysis revealed a significant reprogramming of cardiomyocytes, evident through substantial changes in gene expression. To investigate further these reprogramming changes, we analyzed the expression of selected genes using western blot and RT-qPCR techniques. Utilizing the entire LV of the heart for subsequent assessments, we identified some disparities in gene expression levels, suggesting the involvement of other cell types contributing to the complex process of heart reprogramming induced by CH. This underscores a limitation of our study, highlighting the need for single-cell RNA sequencing to fully establish molecular differences induced by CH linked to specific cell types in the heart. Additionally, it is important to note that the main conclusions of our study are based on a mouse in vivo model. While we anticipate that our findings will be relevant to the human heart, this has not been confirmed.

In conclusion, the recent advance in genetic tools has allowed us to examine the role of the transcriptional factor HIF-1α in mediating the survival of cardiomyocytes during I/R injury. As ischemic heart disease, particularly acute myocardial infarction, remains a leading cause of mortality worldwide, our study brings a clinically important finding that HIF-1 induces beneficial mitophagy, thereby contributes to cardioprotection against I/R injury. Our study not only contributes to our understanding of the pathophysiology of heart disease but also the role of HIF-1 in cardioprotective mechanisms. HIF-1 is a central component of cardioprotective IPC, and therefore, various ways to target the HIF-1 pathway or to supplement HIF downstream target molecules are under active investigation. Stabilization of HIF-1 by IPC or pharmacologic intervention has been tested in recent clinical trials.[71] However, the development of newer intervention agents specifically targeting the HIF-1 pathways is essential. Our finding of HIF-1-mediated mitophagy as a mechanism for cardioprotection against I/R injury represents a new avenue for potentially targeting mitochondrial pathways in the treatment of acute myocardial infarction. Since the underlying molecular mechanisms are complex, further studies are required to identify the specific pathway through which mitophagy can be effectively induced to be cardioprotective and explore its therapeutic applications.

4 | MATERIALS AND METHODS

All chemicals were purchased from Merck, Germany, if not specified otherwise.

4.1 | Animals

All animal experiments were approved by the Animal Care and Use Committees of the Institute of Molecular Genetics and the Institute of Physiology of the Czech Academy of Sciences (Permit Number: 75/2016). Experiments were performed in males, and WT males were compared to *hif1a*$^{+/-}$ males with the *hif1a*^{tm1jhu} null allele.[72] The line was maintained on the FVB background. *hif1a*$^{+/-}$ mice show a partial loss of HIF-1α protein expression levels.[73,74] Mice were kept under standard experimental conditions with constant temperature (23–24°C) and fed on standard diet (Altromin, #1324, Germany). Genotyping was performed by polymerase chain reaction (PCR; Table S5) on tail DNA.[75,76]

4.2 | Chronic hypoxia

Both WT and *hif1a*$^{+/-}$ mice were exposed to intermittent hypobaric hypoxia of 7000 m for 8 h/day, 5 days a week. Barometric pressure was lowered stepwise, so that the final level was reached after 6 exposures. The total number of exposures was 20. The control groups of animals were kept for the same period of time at room air. Mice were terminated on the next day after the last hypoxic exposure.

4.3 | Isolated perfused hearts

Animals were killed by cervical dislocation and hearts were rapidly excised and perfused according to Langendorff under constant pressure of 80 mm Hg with non-recirculating modified Krebs–Henseleit solution (18 mM NaCl, 25 mM $NaHCO_3$, 4.7 mM KCl, 1.2 mM $MgSO_4$, 1.2 mM KH_2PO_4, 2.5 mM $CaCl_2$, 0.5 mM EDTA, 11 mM glucose; Penta Chemicals) gassed with 95% O_2 and 5% CO_2 (pH 7.4) and maintained at 37°C. After 15 min of stabilization, the spontaneously beating hearts were

subjected to 45 min of global no-flow normothermic ischemia followed by 60 min of reperfusion.[77]

In a separate set of experiments, mice were administered with mdivi-1, a mitochondrial fission inhibitor (Merck, M0199; 25 mg/kg body weight, i.p.) or corresponding volume of dimethyl sulfoxide (DMSO) 15 min before sacrificing. Subsequently, we followed the same protocol as described above.

4.4 | Infarct size determination

A 2 mL bolus of 1% 2,3,5 triphenyltetrazolium chloride (TTC; Merck, T8877) was injected through the aorta followed by incubation of the heart in TTC for 30 min at 37°C and fixation overnight in 10% neutral formaldehyde solution. Next day, the RV was separated and the LV was cut perpendicularly to the long axis into 5–6 slices. The IS (TTC-negative) and the size of the LV were determined from photographs by a computerized planimetric method using the software Ellipse (ViDiTo, Slovakia). The IS was normalized to the size of the LV.[77]

4.5 | Tissue processing

Separate groups of animals (not subjected to myocardial I/R injury) assigned to biochemical analyses of the LV myocardium were killed by cervical dislocation, hearts were rapidly excised, washed in cold (0°C) saline, dissected into the RV, the LV, and the septum and weighed; the LV free wall was frozen in liquid nitrogen and stored at −80°C until use.

4.6 | Mitochondrial respiration

Animals were sacrificed, hearts quickly excised and atria were removed. The heart homogenates were prepared on ice in 0.25 M STE buffer [100 mM NaCl, 10 mM Tris–HCl (pH 8.0), 1 mM EDTA] using a glass-teflon homogenizer and filtered through a fine mesh. Detection of protein concentration was performed using the Bradford method. Freshly harvested mitochondria were used for respirometry analyses. Oxygen consumption was detected at 30°C using the Oxygraph-2k (Oroboros Instruments GmbH, Innsbruck, Austria) as previously described.[78,79] Respiration was measured in the XFe MAS medium (220 mM mannitol, 70 mM sucrose, 10 mM KH_2PO_4, 5 mM $MgCl_2$, 2 mM HEPES, 3 mM EGTA, 0.2% bovine serum albumin). Substrates and inhibitors were added in following order and concentrations: 50 µM palmitoyl carnitine, 2 mM malate, 1 mM ADP, 5 µM cytochrome *c*, 10 mM pyruvate, 10 mM glutamate, 10 mM succinate, 1 µM oligomycin, 500 nM carbonyl cyanide p-trifluoro-methoxyphenyl hydrazone—FCCP titration, 0.5 µM rotenone, 10 mM malonate, 2 mM ascorbate, 1 mM *N*,*N*,*N*′,*N*′-tetramethylphenylenediamine (TPMD), 0.5 mM KCN. Data were expressed as pmol O_2/s/mg protein.

4.7 | Mitochondrial DNA content

Mitochondrial DNA was quantified using a comparative Ct method, taking the ratio between a target mitochondrial gene and a reference nuclear gene using qPCR. Briefly, total DNA from LV of 12-week-old mice was isolated by TRIzol Reagent (Invitrogen, 15596026) using the interphase and lower phenol–chloroform phase according to the manufacturer's protocol. Obtained total DNA was quantified by Nanodrop 2000 (Thermo Fisher Scientific, Waltham, MA, USA). The qPCR was performed on QuantStudio 5 (Thermo Fisher Scientific, Waltham, MA, USA) using Power SyberGreen PCR Master Mix (Thermo Fisher Scientific, 4367659). Amount of mtDNA was measured using primers against mitochondrially encoded *Mtatp6* gene and nuclear-encoded *Nme1* gene.[80] Primer sequences are presented in Table S4.

4.8 | Transmission electron microscopy

The samples for TEM were obtained from the freshly excised hearts. The cross sections of the LV anterior walls were fixed in 2.5% glutaraldehyde in 0.1 M sodium cacodylate buffer (pH 7.4) at 4°C. After an overnight incubation, the fixative was replaced with fresh buffer and kept at 4°C. The samples were then with buffer at 4°C, stained in 1% osmium tetroxide (OsO_4) with 1% potassium ferrocyanide ($K_4Fe(CN)_6$) in 0.1 M sodium cacodylate buffer (pH 7.4) for 1 h at 4°C, embedded in resin and sectioned. After washing 3 × 5 min with ddH_2O at 4°C, the samples were dehydrated in a graded ethanol series and embedded in polymerized resin. Tissues were sectioned using an Ultrotome V (LKB, Stockholm, Sweden). Ultrathin sections were examined with FEI Tecnai G2 transmission electron microscope (FEI, Hillsboro, OR, USA). ImageJ (Java Technology, CA, USA) was used to measure the area of the mitochondria in micrographs.[81]

4.9 | CRISPR-Cas9 in AC16 cell line

The AC16 cells were maintained in growth medium DMEM/Nutrient Mixture F-12 (Thermo Fisher

Scientific, 11320033) at 37°C in a humidified atmosphere of 5% CO_2. Cells were subcultured until 70% confluence then divided. The *Atg7* KO cell lines in AC16 background were generated by CRISPR-Cas9 technology according to Zhang laboratory protocol[82] using px458 plasmid (Addgene 48138). AC16 WT cells and *Atg7* KO cells were transfected either with proline hydroxylases resistant HA-HIF1alpha P402A/P564A-pcDNA3 plasmid (Addgene, 18955) or empty vector pcDNA3.1 by GenJet In Vitro DNA Transfection Reagent (SigmaGen Laboratories, SL100489) resulting in HIF-1α overexpression. After 72 h, cell lysates were prepared for western blot.

4.10 | Western blotting

The LV tissue samples were disrupted by TissueLyser in eight volumes of ice-cold homogenization buffer [12.5 mM Tris (pH 7.4), 250 mM sucrose, 2.5 mM EGTA, 1 mM EDTA, 6 mM β-mercaptoethanol, protease (Merck, 04693159001) and phosphatase (Merck, 04906837001) inhibitors]. Lysates were centrifuged for 10 min at 10000*g* at 4°C. Supernatant aliquots were stored at −80°C until use. Total protein concentrations were determined using the Bradford protein assay. Lysates were separated by sodium dodecyl-sulfate polyacrylamide gel electrophoresis (SDS-PAGE, 10 or 15% gels) and transferred to polyvinylidene difluoride membranes (Bio-Rad, 1620177). After blocking with 5% dry low-fat milk in Tween-20 Tris-base sodium buffer for 1 h at room temperature, membranes were washed and probed at 4°C with the following primary antibodies against: ATG7 (Abcam, ab133528), ATP5B (Abcam, ab14730), COX1 (Abcam, ab110413; 1:1000), LC3 (Abcam, ab128025; 1:1000), LDHA (Rockland, 100–1173, 1:1000), PINK1 (Cayman Chemicals, 10006283; 1:1000), SQSTM1/p62 (Cell Signaling Technology, 23214s; 1:1000). After overnight incubation, the membranes were washed and incubated for 1 h at room temperature with fluorescent secondary antibodies Alexa Fluor 680 (Invitrogen, A10038 and A10043; 1:10000). The bands were visualized by Odyssey CLx (LI-COR Biosciences, Lincoln, NE, USA) and quantified using ImageJ software (Java Technology, Cupertino, CA). The samples from each experimental group were run on the same gel and quantified on the same membrane. Since the expressions of commonly used loading controls such as glyceraldehyde 3-phosphatase dehydrogenase or β-actin are affected by adaptation to CH,[58] vinculin (Merck, V4139; 1:5000) served as a loading control for our western blot experiments.

LC3 immunoblotting was performed in the presence and absence of lysosomal inhibitor to accurately evaluate the total autophagic flux. Leupeptin (Merck, L2884; 40 mg/kg body weight) or corresponding volume of PBS were administered to mice via intraperitoneal injection and the animals were sacrificed 1 h thereafter.[83] We defined autophagic flux as the increase in the lipidated LC3-II that was induced by the addition of inhibitor.

4.11 | Adult mouse cardiomyocytes isolation

Adult mouse LV myocytes were isolated according to Kaludercic et al.[52] with minor modifications. Briefly, the 12-week-old mice were pretreated with heparin (Zentiva, 08594739026131; 40 IU/g body weight, i.p.) and rapidly sacrificed by cervical dislocation. The hearts were excised and perfused with a calcium-free perfusion buffer to clean it from blood and arrest contraction, followed by a solution containing collagenase (Worthington, LS004177) and protease (Merck, P5147) enzymes to digest the extracellular matrix. After digestion, atria and RV were removed and LV myocytes were dispersed into a single-cell suspension and centrifuged (100*g*, 1 min, 25°C). Supernatant was replaced and TRIzol (Invitrogen, 15596026) was added and resuspended with the cell suspension. Prior to RNA isolation, the samples were stored at −80°C.

4.12 | RNA-sequencing

Total RNA was extracted from the LV cardiomyocytes of 12-week-old mice. Fragment Analyzer assessed the quality of cDNA libraries. The libraries were prepared using kit SureSelect XT HS2 mRNA Library Preparation System with Poly A Selection (Agilent) and sequenced on an Illumina NextSeq 500 next-generation sequencer. NextSeq 500/550 High Output kit 75 cycles (Illumina, 200024906) were processed at the Genomics and Bioinformatics Core Facility (Institute of Molecular Genetics CAS, Czechia). RNA-Seq reads in FASTQ files were mapped to the mouse genome using STAR [version 2.7.0c[84]] GRCm38 primary assembly and annotation version M8. The raw data of RNA sequencing were processed with a standard pipeline. Using cutadapt v1.18,[85] the number of reads (minimum, 32 million; maximum, 73 million) was trimmed by Illumina sequencing adaptor and of bases with reading quality lower than 20, subsequently reads shorter than 20 b< were filtered out. TrimmomaticPE version 0.36.[86] Ribosomal RNA and reads mapping to UniVec database

were filtered out using boWTie v1.2.2. with parameters -S -n 1 and SortMeRNA.[87] A count table was generated by Rsubread v2.0.1 package using default parameters without counting multi mapping reads. The raw RNA-seq data were deposited at GEO: (https://www.ncbi.nlm.nih.gov/geo/).[88]

DESeq2 [v1.26.0[89]] default parameters were used to normalize data and compare the different groups. Genes were then filtered using the criteria an adjusted *p*-value $p_{adj} < 0.05$, and a base mean ≥50, and a 30%-fold change threshold. The enrichment of the functional categories and functional annotation clustering of the differentially expressed genes was performed using g: Profiler[90] input using version e104_eg51_p15_3922dba with g: SCS multiple testing correction methods applying a significance threshold of 0.05. Complete query details are available in Query info tabs in Dataset S2. The resulting GEM and combined GMT files were loaded into Cytoscape plugin "EnrichmentMap" using 0.01 FDR q-value cutoff to generate a network.

4.13 | Reverse transcription-quantitative real-time polymerase chain reaction

Total RNA was isolated from the LV of 12-week-old mice ($n = 6$ samples/group). Following reverse transcription with 1 μg of total RNA, qPCR was performed with the initial AmpliTaq activation at 95°C for 10 min, followed by 40 cycles at 95°C for 15 s and 60°C for 30 s, as described.[91] The *Hprt1* gene was selected as the best reference gene for our analyses from a panel of 12 control genes (TATAA Biocenter AB, Sweden).[92] The relative expression of a target gene was calculated, based on qPCR efficiencies and the quantification cycle (Cq) difference (Δ) of an experimental sample versus control. Primers were designed using the Primer Blast tool (https://www.ncbi.nlm.nih.gov/tools/primer-blast/). Primers were selected according to the following parameters: length between 18 and 24 bases, melting temperature (Tm) between 58° and 60°C, G + C content between 40% and 60% (optimal 50%) and efficiency above 80%. Primer sequences are presented in Table S4.

4.14 | Statistical analysis

Statistical analyses were performed using GraphPad Prism 8 software (Graph Pad Inc., CA, USA). Two-way analysis of variance (ANOVA; with genotype and experimental conditions as categories) or three-way ANOVA (with genotype, experimental conditions and treatment as categories) were carried out to determine significant interactions, followed by a recommended post-hoc test for multiple comparisons. Values are expressed as mean ± SEM or SD (when $n < 7$). Statistical significance is indicated by symbols $^{*}p < 0.05$, $^{\dagger}p < 0.01$, $^{\ddagger}p < 0.001$.

5 | CONCLUSION

In summary, our findings provide the supporting evidence that HIF-1α stabilized under the conditions of chronic hypoxia enhances degradation of possibly harmful mitochondria by activating mitophagy and thus, boosts the development of the cardioprotective phenotype.

AUTHOR CONTRIBUTIONS

Petra Alanova: Conceptualization; investigation; funding acquisition; writing – original draft; methodology; writing – review and editing; project administration; supervision; validation. **Lukas Alan:** Investigation; methodology; funding acquisition; validation; writing – original draft; writing – review and editing. **Barbora Opletalova:** Investigation; funding acquisition; methodology; validation. **Romana Bohuslavova:** Investigation; writing – original draft; writing – review and editing; methodology; project administration; validation. **Pavel Abaffy:** Investigation; methodology; software; validation. **Katerina Matejkova:** Investigation; methodology; validation. **Kristyna Holzerova:** Investigation. **Daniel Benak:** Investigation. **Nina Kaludercic:** Methodology; writing – review and editing. **Roberta Menabo:** Writing – review and editing; methodology. **Fabio Di Lisa:** Writing – review and editing; methodology. **Bohuslav Ostadal:** Writing – review and editing. **Frantisek Kolar:** Writing – review and editing; supervision; writing – original draft; funding acquisition. **Gabriela Pavlinkova:** Conceptualization; writing – original draft; supervision; project administration; funding acquisition; investigation; writing – review and editing.

ACKNOWLEDGMENTS

This research was supported by the Ministry of Health of the Czech Republic, grant no. NU20J-02-00035; the project National Institute for Research of Metabolic and Cardiovascular Diseases (Programme EXCELES, ID Project No. LX22NPO5104) – Funded by the European Union – Next Generation EU; Charles University, project GA UK No 270623; and by institutional funding Czech Academy of Sciences RVO: 86652036. LA is the recipient of the MSCA_0000019, MUR Concession Decree No. n. 564 of December 13, 2022, CUP C93C22007550006 funded under the National Recovery and Resilience Plan

(NRRP), Mission 4, Component 2, Investment 1.2, MUR Call for tender n. 367 of October 7, 2022 funded by the European Union – Next Generation EU. Graphical illustrations were created with BioRender.com. We acknowledge BIOCEV GeneCore Facility for its support with gene expression/transcriptome analyses; and BIOCEV Animal facility (LM 2018126 Czech Centre for Phenogenomics by MEYS OP RDE CZ.02.1.01/0.0/0.0/18_046/0015861 CCP Infrastructure Upgrade II by MEYS and ESIF). Open access publishing facilitated by Fyziologicky ustav Akademie ved Ceske republiky, as part of the Wiley - CzechELib agreement.

CONFLICT OF INTEREST STATEMENT

No potential conflict of interest was reported by the author(s).

DATA AVAILABILITY STATEMENT

The data that support the findings of this study are openly available in GEO repository at https://www.ncbi.nlm.nih.gov/geo under accession number GSE255797.

ORCID

Petra Alanova https://orcid.org/0000-0001-9900-7074

REFERENCES

1. Anderson JD, Honigman B. The effect of altitude-induced hypoxia on heart disease: do acute, intermittent, and chronic exposures provide cardioprotection? *High Alt Med Biol*. 2011;12(1):45-55. doi:10.1089/ham.2010.1021
2. Hurtado A. Some clinical aspects of life at high altitudes. *Ann Intern Med*. 1960;53:247-258. doi:10.7326/0003-4819-53-2-247
3. Ostadal B, Kolar F. Cardiac adaptation to chronic high-altitude hypoxia: beneficial and adverse effects. *Respir Physiol Neurobiol*. 2007;158(2–3):224-236. doi:10.1016/j.resp.2007.03.005
4. Ostádal B, Kolár F, Pelouch V, Widimský J. Ontogenetic differences in cardiopulmonary adaptation to chronic hypoxia. *Physiol Res*. 1995;44(1):45-51. PubMed PMID: 8789299; eng.
5. Semenza GL. Targeting HIF-1 for cancer therapy. *Nat Rev Cancer*. 2003;3(10):721-732. doi:10.1038/nrc1187
6. Semenza GL. HIF-1, O(2), and the 3 PHDs: how animal cells signal hypoxia to the nucleus. *Cell*. 2001;107(1):1-3. doi:10.1016/s0092-8674(01)00518-9
7. Wang GL, Jiang BH, Rue EA, Semenza GL. Hypoxia-inducible factor 1 is a basic-helix-loop-helix-PAS heterodimer regulated by cellular O2 tension. *Proc Natl Acad Sci USA*. 1995;92(12):5510-5514. doi:10.1073/pnas.92.12.5510
8. Cai Z, Zhong H, Bosch-Marce M, et al. Complete loss of ischaemic preconditioning-induced cardioprotection in mice with partial deficiency of HIF-1 alpha. *Cardiovasc Res*. 2008;77(3):463-470. doi:10.1093/cvr/cvm035
9. Cai Z, Luo W, Zhan H, Semenza GL. Hypoxia-inducible factor 1 is required for remote ischemic preconditioning of the heart. *Proc Natl Acad Sci USA*. 2013;110(43):17462-17467. doi:10.1073/pnas.1317158110
10. Neckár J, Ostádal B, Kolár F. Myocardial infarct size-limiting effect of chronic hypoxia persists for five weeks of normoxic recovery. *Physiol Res*. 2004;53(6):621-628.
11. Semenza GL. O_2-regulated gene expression: transcriptional control of cardiorespiratory physiology by HIF-1. *J Appl Physiol*. 2004;96(3):1173-1177; discussion 1170–2. doi:10.1152/japplphysiol.00770.2003
12. Essop MF. Cardiac metabolic adaptations in response to chronic hypoxia. *J Physiol*. 2007;584(Pt 3):715-726. doi:10.1113/jphysiol.2007.143511
13. Schaper J, Meiser E, Stämmler G. Ultrastructural morphometric analysis of myocardium from dogs, rats, hamsters, mice, and from human hearts. *Circ Res*. 1985;56(3):377-391. doi:10.1161/01.res.56.3.377
14. Murphy E, Steenbergen C. Regulation of mitochondrial Ca(2+) uptake. *Annu Rev Physiol*. 2021;83:107-126. doi:10.1146/annurev-physiol-031920-092419
15. Janssen-Heininger YM, Mossman BT, Heintz NH, et al. Redox-based regulation of signal transduction: principles, pitfalls, and promises. *Free Radic Biol Med*. 2008;45(1):1-17. doi:10.1016/j.freeradbiomed.2008.03.011
16. Asemu G, Papousek F, Ostádal B, et al. Adaptation to high altitude hypoxia protects the rat heart against ischemia-induced arrhythmias. Involvement of mitochondrial K(ATP) channel. *J Mol Cell Cardiol*. 1999;31(10):1821-1831. doi:10.1006/jmcc.1999.1013
17. Borchert GH, Yang C, Kolár F. Mitochondrial BKCa channels contribute to protection of cardiomyocytes isolated from chronically hypoxic rats. *Am J Physiol Heart Circ Physiol*. 2011;300(2):H507-H513. doi:10.1152/ajpheart.00594.2010
18. Mizushima N, Komatsu M. Autophagy: renovation of cells and tissues. *Cell*. 2011;147(4):728-741. doi:10.1016/j.cell.2011.10.026
19. Saito T, Sadoshima J. Molecular mechanisms of mitochondrial autophagy/mitophagy in the heart. *Circ Res*. 2015;116(8):1477-1490. doi:10.1161/circresaha.116.303790
20. Alánová P, Chytilová A, Neckář J, et al. Myocardial ischemic tolerance in rats subjected to endurance exercise training during adaptation to chronic hypoxia. *J Appl Physiol*. 2017;122(6):1452-1461. doi:10.1152/japplphysiol.00671.2016
21. Gustafsson AB, Gottlieb RA. Bcl-2 family members and apoptosis, taken to heart. *Am J Physiol Cell Physiol*. 2007;292(1):C45-C51. doi:10.1152/ajpcell.00229.2006
22. Honkoop H, de Bakker DE, Aharonov A, et al. Single-cell analysis uncovers that metabolic reprogramming by ErbB2 signaling is essential for cardiomyocyte proliferation in the regenerating heart. *elife*. 2019;8:e50163. doi:10.7554/eLife.50163
23. Ahuja P, Zhao P, Angelis E, et al. Myc controls transcriptional regulation of cardiac metabolism and mitochondrial biogenesis in response to pathological stress in mice. *J Clin Invest*. 2010;120(5):1494-1505. doi:10.1172/JCI38331
24. Khachigian LM. Early growth response-1 in cardiovascular pathobiology. *Circ Res*. 2006;98(2):186-191. doi:10.1161/01.RES.0000200177.53882.c3
25. Harhous Z, Booz GW, Ovize M, Bidaux G, Kurdi M. An update on the multifaceted roles of STAT3 in the heart. *Front Cardiovasc Med*. 2019;6:150. doi:10.3389/fcvm.2019.00150
26. Thu VT, Kim HK, Ha SH, et al. Glutathione peroxidase 1 protects mitochondria against hypoxia/reoxygenation damage in mouse hearts. *Pflugers Arch*. 2010;460(1):55-68. doi:10.1007/s00424-010-0811-7
27. Wang H, Wang L, Hu F, et al. Neuregulin-4 attenuates diabetic cardiomyopathy by regulating autophagy via the AMPK/

mTOR signalling pathway. *Cardiovasc Diabetol*. 2022;21(1):205. doi:10.1186/s12933-022-01643-0
28. Gao S, Li G, Shao Y, et al. FABP5 deficiency impairs mitochondrial function and aggravates pathological cardiac remodeling and dysfunction. *Cardiovasc Toxicol*. 2021;21(8):619-629. doi:10.1007/s12012-021-09653-2
29. Zhang J, Qiao C, Chang L, et al. Cardiomyocyte overexpression of FABP4 aggravates pressure overload-induced heart hypertrophy. *PLoS One*. 2016;11(6):e0157372. doi:10.1371/journal.pone.0157372
30. Pankiv S, Clausen TH, Lamark T, et al. p62/SQSTM1 binds directly to Atg8/LC3 to facilitate degradation of ubiquitinated protein aggregates by autophagy. *J Biol Chem*. 2007;282(33):24131-24145. doi:10.1074/jbc.M702824200
31. Okatsu K, Uno M, Koyano F, et al. A dimeric PINK1-containing complex on depolarized mitochondria stimulates Parkin recruitment. *J Biol Chem*. 2013;288(51):36372-36384. doi:10.1074/jbc.M113.509653
32. Lazarou M, Jin SM, Kane LA, Youle RJ. Role of PINK1 binding to the TOM complex and alternate intracellular membranes in recruitment and activation of the E3 ligase Parkin. *Dev Cell*. 2012;22(2):320-333. doi:10.1016/j.devcel.2011.12.014
33. Yan Q, Bartz S, Mao M, Li L, Kaelin WG Jr. The hypoxia-inducible factor 2alpha N-terminal and C-terminal transactivation domains cooperate to promote renal tumorigenesis in vivo. *Mol Cell Biol*. 2007;27(6):2092-2102. doi:10.1128/mcb.01514-06
34. Firth JD, Ebert BL, Pugh CW, Ratcliffe PJ. Oxygen-regulated control elements in the phosphoglycerate kinase 1 and lactate dehydrogenase A genes: similarities with the erythropoietin 3′ enhancer. *Proc Natl Acad Sci USA*. 1994;91(14):6496-6500. doi:10.1073/pnas.91.14.6496
35. Collier JJ, Guissart C, Oláhová M, et al. Developmental consequences of defective ATG7-mediated autophagy in humans. *N Engl J Med*. 2021;384(25):2406-2417. doi:10.1056/NEJMoa1915722
36. Youle RJ, van der Bliek AM. Mitochondrial fission, fusion, and stress. *Science (New York, NY)*. 2012;337(6098):1062-1065. doi:10.1126/science.1219855
37. Kim H, Lee JY, Park KJ, Kim WH, Roh GS. A mitochondrial division inhibitor, Mdivi-1, inhibits mitochondrial fragmentation and attenuates kainic acid-induced hippocampal cell death. *BMC Neurosci*. 2016;17(1):33. doi:10.1186/s12868-016-0270-y
38. Béguin PC, Joyeux-Faure M, Godin-Ribuot D, et al. Acute intermittent hypoxia improves rat myocardium tolerance to ischemia. *J Appl Physiol*. 2005;99(3):1064-1069. doi:10.1152/japplphysiol.00056.2005
39. Neckár J, Szárszoi O, Koten L, et al. Effects of mitochondrial K(ATP) modulators on cardioprotection induced by chronic high altitude hypoxia in rats. *Cardiovasc Res*. 2002;55(3):567-575. doi:10.1016/s0008-6363(02)00456-x
40. Asemu G, Neckár J, Szárszoi O, Papousek F, Ostádal B, Kolar F. Effects of adaptation to intermittent high altitude hypoxia on ischemic ventricular arrhythmias in rats. *Physiol Res*. 2000;49(5):597-606.
41. Zhang R, Yang A, Zhang L, et al. MFN2 deficiency promotes cardiac response to hypobaric hypoxia by reprogramming cardiomyocyte metabolism. *Acta Physiol (Oxf)*. 2023;239(1):e14018. doi:10.1111/apha.14018
42. Fähling M, Mathia S, Paliege A, et al. Tubular von Hippel-Lindau knockout protects against rhabdomyolysis-induced AKI. *J Am Soc Nephrol*. 2013;24(11):1806-1819. doi:10.1681/asn.2013030281
43. Cai Z, Manalo DJ, Wei G, et al. Hearts from rodents exposed to intermittent hypoxia or erythropoietin are protected against ischemia-reperfusion injury. *Circulation*. 2003;108(1):79-85. doi:10.1161/01.Cir.0000078635.89229.8a
44. Yang L, Xie P, Wu J, et al. Sevoflurane postconditioning improves myocardial mitochondrial respiratory function and reduces myocardial ischemia-reperfusion injury by up-regulating HIF-1. *Am J Transl Res*. 2016;8(10):4415-4424.
45. Zhao HX, Wang XL, Wang YH, et al. Attenuation of myocardial injury by postconditioning: role of hypoxia inducible factor-1alpha. *Basic Res Cardiol*. 2010;105(1):109-118. doi:10.1007/s00395-009-0044-0
46. Jezková J, Nováková O, Kolár F, et al. Chronic hypoxia alters fatty acid composition of phospholipids in right and left ventricular myocardium. *Mol Cell Biochem*. 2002;232(1–2):49-56. doi:10.1023/a:1014889115509
47. Thompson LP, Song H, Polster BM. Fetal programming and sexual dimorphism of mitochondrial protein expression and activity of hearts of prenatally hypoxic Guinea pig offspring. *Oxidative Med Cell Longev*. 2019;2019:7210249.
48. Zhang H, Bosch-Marce M, Shimoda LA, et al. Mitochondrial autophagy is an HIF-1-dependent adaptive metabolic response to hypoxia. *J Biol Chem*. 2008;283(16):10892-10903. doi:10.1074/jbc.M800102200
49. Murphy MP. How mitochondria produce reactive oxygen species. *Biochem J*. 2009;417(1):1-13. doi:10.1042/bj20081386
50. Cadenas E, Davies KJ. Mitochondrial free radical generation, oxidative stress, and aging. *Free Radic Biol Med*. 2000;29(3–4):222-230. doi:10.1016/s0891-5849(00)00317-8
51. Bianchi P, Kunduzova O, Masini E, et al. Oxidative stress by monoamine oxidase mediates receptor-independent cardiomyocyte apoptosis by serotonin and postischemic myocardial injury. *Circulation*. 2005;112(21):3297-3305. doi:10.1161/circulationaha.104.528133
52. Kaludercic N, Carpi A, Nagayama T, et al. Monoamine oxidase B prompts mitochondrial and cardiac dysfunction in pressure overloaded hearts. *Antioxid Redox Signal*. 2014;20(2):267-280. doi:10.1089/ars.2012.4616
53. Kaludercic N, Takimoto E, Nagayama T, et al. Monoamine oxidase A-mediated enhanced catabolism of norepinephrine contributes to adverse remodeling and pump failure in hearts with pressure overload. *Circ Res*. 2010;106(1):193-202. doi:10.1161/circresaha.109.198366
54. Cagnin S, Brugnaro M, Millino C, et al. Monoamine oxidase-dependent pro-survival signaling in diabetic hearts is mediated by miRNAs. *Cells*. 2022;11(17):2697. doi:10.3390/cells11172697
55. Deshwal S, Forkink M, Hu CH, et al. Monoamine oxidase-dependent endoplasmic reticulum-mitochondria dysfunction and mast cell degranulation lead to adverse cardiac remodeling in diabetes. *Cell Death Differ*. 2018;25(9):1671-1685. doi:10.1038/s41418-018-0071-1
56. Antonucci S, Di Sante M, Tonolo F, et al. The determining role of mitochondrial reactive oxygen species generation and monoamine oxidase activity in doxorubicin-induced cardiotoxicity. *Antioxid Redox Signal*. 2021;34(7):531-550. doi:10.1089/ars.2019.7929
57. Míčová P, Klevstig M, Holzerová K, et al. Antioxidant tempol suppresses heart cytosolic phospholipase A(2)α stimulated

by chronic intermittent hypoxia. *Can J Physiol Pharmacol*. 2017;95(8):920-927. doi:10.1139/cjpp-2017-0022
58. Balková P, Hlaváčková M, Milerová M, et al. N-acetylcysteine treatment prevents the up-regulation of MnSOD in chronically hypoxic rat hearts. *Physiol Res*. 2011;60(3):467-474. doi:10.33549/physiolres.932042
59. Twig G, Elorza A, Molina AJ, et al. Fission and selective fusion govern mitochondrial segregation and elimination by autophagy. *EMBO J*. 2008;27(2):433-446. doi:10.1038/sj.emboj.7601963
60. Gomes LC, Di Benedetto G, Scorrano L. During autophagy mitochondria elongate, are spared from degradation and sustain cell viability. *Nat Cell Biol*. 2011;13(5):589-598. doi:10.1038/ncb2220
61. Giacomello M, Pyakurel A, Glytsou C, Scorrano L. The cell biology of mitochondrial membrane dynamics. *Nat Rev Mol Cell Biol*. 2020;21(4):204-224. doi:10.1038/s41580-020-0210-7
62. Alan L, Scorrano L. Shaping fuel utilization by mitochondria. *Curr Biol*. 2022;32(12):R618-R623. doi:10.1016/j.cub.2022.05.006
63. Prabu SK, Anandatheerthavarada HK, Raza H, Srinivasan S, Spear JF, Avadhani NG. Protein kinase A-mediated phosphorylation modulates cytochrome c oxidase function and augments hypoxia and myocardial ischemia-related injury. *J Biol Chem*. 2006;281(4):2061-2070. doi:10.1074/jbc.M507741200
64. Menzies RA, Gold PH. The turnover of mitochondria in a variety of tissues of young adult and aged rats. *J Biol Chem*. 1971;246(8):2425-2429.
65. Sciarretta S, Maejima Y, Zablocki D, Sadoshima J. The role of autophagy in the heart. *Annu Rev Physiol*. 2018;80:1-26. doi:10.1146/annurev-physiol-021317-121427
66. Titus AS, Sung EA, Zablocki D, Sadoshima J. Mitophagy for cardioprotection. *Basic Res Cardiol*. 2023;118(1):42. doi:10.1007/s00395-023-01009-x
67. Zhu H, Wang D, Liu Y, et al. Role of the Hypoxia-inducible factor-1 alpha induced autophagy in the conversion of non-stem pancreatic cancer cells into CD133+ pancreatic cancer stem-like cells. *Cancer Cell Int*. 2013;13(1):119. doi:10.1186/1475-2867-13-119
68. Guo H, Ding H, Yan Y, et al. Intermittent hypoxia-induced autophagy via AMPK/mTOR signaling pathway attenuates endothelial apoptosis and dysfunction in vitro. *Sleep Breath*. 2021;25(4):1859-1865. doi:10.1007/s11325-021-02297-0
69. Semenza GL. Mitochondrial autophagy: life and breath of the cell. *Autophagy*. 2008;4(4):534-536. doi:10.4161/auto.5956
70. Ma X, Godar RJ, Liu H, Diwan A. Enhancing lysosome biogenesis attenuates BNIP3-induced cardiomyocyte death. *Autophagy*. 2012;8(3):297-309. doi:10.4161/auto.18658
71. Lee JW, Ko J, Ju C, Eltzschig HK. Hypoxia signaling in human diseases and therapeutic targets. *Exp Mol Med*. 2019;51(6):1-13. doi:10.1038/s12276-019-0235-1
72. Iyer NV, Kotch LE, Agani F, et al. Cellular and developmental control of O_2 homeostasis by hypoxia-inducible factor 1 alpha. *Genes Dev*. 1998;12(2):149-162. doi:10.1101/gad.12.2.149
73. Bosch-Marce M, Okuyama H, Wesley JB, et al. Effects of aging and hypoxia-inducible factor-1 activity on angiogenic cell mobilization and recovery of perfusion after limb ischemia. *Circ Res*. 2007;101(12):1310-1318. doi:10.1161/circresaha.107.153346
74. Li J, Bosch-Marce M, Nanayakkara A, et al. Altered metabolic responses to intermitternt hypoxia in mice with partial deficiency of hypoxia-inducible factor 1 a. *Physiol Genomics*. 2006;25:450-457.
75. Bohuslavova R, Skvorova L, Sedmera D, Semenza GL, Pavlinkova G. Increased susceptibility of HIF-1α heterozygous-null mice to cardiovascular malformations associated with maternal diabetes. *J Mol Cell Cardiol*. 2013;60:129-141. doi:10.1016/j.yjmcc.2013.04.015
76. Bohuslavova R, Kolar F, Sedmera D, et al. Partial deficiency of HIF-1α stimulates pathological cardiac changes in streptozotocin-induced diabetic mice. *BMC Endocr Disord*. 2014;14:11. doi:10.1186/1472-6823-14-11
77. Slámová K, Papoušek F, Janovská P, Kopecký J, Kolář F. Adverse effects of AMP-activated protein kinase alpha2-subunit deletion and high-fat diet on heart function and ischemic tolerance in aged female mice. *Physiol Res*. 2016;65(1):33-42. doi:10.33549/physiolres.932979
78. Pecina P, Capková M, Chowdhury SK, et al. Functional alteration of cytochrome c oxidase by SURF1 mutations in Leigh syndrome. *Biochim Biophys Acta*. 2003;1639(1):53-63. doi:10.1016/s0925-4439(03)00127-3
79. Chowdhury SK, Drahota Z, Floryk D, et al. Activities of mitochondrial oxidative phosphorylation enzymes in cultured amniocytes. *Clin Chim Acta*. 2000;298(1–2):157-173. doi:10.1016/s0009-8981(00)00300-4
80. Rey S, Luo W, Shimoda LA, Semenza GL. Metabolic reprogramming by HIF-1 promotes the survival of bone marrow-derived angiogenic cells in ischemic tissue. *Blood*. 2011;117(18):4988-4998. doi:10.1182/blood-2010-11-321190
81. Bean C, Audano M, Varanita T, et al. The mitochondrial protein Opa1 promotes adipocyte browning that is dependent on urea cycle metabolites. *Nat Metab*. 2021;3(12):1633-1647. doi:10.1038/s42255-021-00497-2
82. Ran FA, Hsu PD, Wright J, Agarwala V, Scott DA, Zhang F. Genome engineering using the CRISPR-Cas9 system. *Nat Protoc*. 2013;8(11):2281-2308. doi:10.1038/nprot.2013.143
83. Haspel J, Shaik RS, Ifedigbo E, et al. Characterization of macroautophagic flux in vivo using a leupeptin-based assay. *Autophagy*. 2011;7(6):629-642. doi:10.4161/auto.7.6.15100
84. Dobin A, Davis CA, Schlesinger F, et al. STAR: ultrafast universal RNA-seq aligner. *Bioinformatics (Oxford, England)*. 2013;29(1):15-21. doi:10.1093/bioinformatics/bts635
85. Martin M. Cutadapt removes adapter sequences from high-throughput sequencing reads. *EMBnetjournal*. 2011;17(1):3. doi:10.14806/ej.17.1.200
86. Bolger AM, Lohse M, Usadel B. Trimmomatic: a flexible trimmer for Illumina sequence data. *Bioinformatics (Oxford, England)*. 2014;30(15):2114-2120. doi:10.1093/bioinformatics/btu170
87. Kopylova E, Noé L, Touzet H. SortMeRNA: fast and accurate filtering of ribosomal RNAs in metatranscriptomic data. *Bioinformatics (Oxford, England)*. 2012;28(24):3211-3217. doi:10.1093/bioinformatics/bts611
88. Alanova P, Alan L, Opletalova B, et al. GEO repository at. 2024 https://www.ncbi.nlm.nih.gov/geo; GSE255797
89. Love MI, Huber W, Anders S. Moderated estimation of fold change and dispersion for RNA-seq data with DESeq2. *Genome Biol*. 2014;15(12):550. doi:10.1186/s13059-014-0550-8
90. Raudvere U, Kolberg L, Kuzmin I, et al. g:profiler: a web server for functional enrichment analysis and conversions of gene lists (2019 update). *Nucleic Acids Res*. 2019;47(W1):W191-W198. doi:10.1093/nar/gkz369

91. Bohuslavová R, Kolář F, Kuthanová L, et al. Gene expression profiling of sex differences in HIF1-dependent adaptive cardiac responses to chronic hypoxia. *J Appl Physiol*. 2010;109(4):1195-1202. doi:10.1152/japplphysiol.00366.2010
92. Benak D, Sotakova-Kasparova D, Neckar J, Kolar F, Hlavackova M. Selection of optimal reference genes for gene expression studies in chronically hypoxic rat heart. *Mol Cell Biochem*. 2019;461(1–2):15-22. doi:10.1007/s11010-019-03584-x

SUPPORTING INFORMATION

Additional supporting information can be found online in the Supporting Information section at the end of this article.

How to cite this article: Alanova P, Alan L, Opletalova B, et al. HIF-1α limits myocardial infarction by promoting mitophagy in mouse hearts adapted to chronic hypoxia. *Acta Physiol*. 2024;240:e14202. doi:10.1111/apha.14202